

Competition and facilitation between unicellular nitrogen-fixing cyanobacteria and non-nitrogen-fixing phytoplankton species

Nona S. R. Agawin¹

Aquatic Microbiology, Institute for Biodiversity and Ecosystem Dynamics, University of Amsterdam, Nieuwe Achtergracht 127, 1018 WS Amsterdam, The Netherlands

Sophie Rabouille

Ocean Sciences Department, University of California at Santa Cruz, Santa Cruz, California 95064

Marcel J. W. Veldhuis

Royal Netherlands Institute for Sea Research, P.O. Box 59, 1790 AB Den Burg, The Netherlands

Lidewij Servatius, Suzanne Hol, Harriët M. J. van Overzee, and Jef Huisman²

Aquatic Microbiology, Institute for Biodiversity and Ecosystem Dynamics, University of Amsterdam, Nieuwe Achtergracht 127, 1018 WS Amsterdam, The Netherlands

Abstract

Recent discoveries show that small unicellular nitrogen-fixing cyanobacteria are more widespread than previously thought and can make major contributions to the nitrogen budget of the oceans. We combined theory and experiments to investigate competition for nitrogen and light between these small unicellular diazotrophs and other phytoplankton species. We developed a competition model that incorporates several physiological processes, including the light dependence of nitrogen fixation, the switch between nitrate assimilation and nitrogen fixation, and the release of fixed nitrogen. Model predictions were tested in nitrogen-limited and light-limited chemostat experiments using the unicellular nitrogen-fixing cyanobacterium *Cyanothece* sp. Miami BG 043511, the picocyanobacterium *Synechococcus bacillaris* CCMP 1333, and the small green alga *Chlorella*_cf sp. CCMP 1227. Parameter values of the species were estimated by calibration of the model in monoculture experiments. The model predictions were subsequently tested in a series of competition experiments at different nitrate levels. The model predictions were generally in good agreement with observed population dynamics. As predicted, in experiments with high nitrate input concentrations, the species with lowest critical light intensity (*S. bacillaris*) competitively excluded the other species. At low nitrate input concentration, nitrogen release by *Cyanothece* enabled stable coexistence of *Cyanothece* and *S. bacillaris*. More specifically, model simulations predicted that fixed nitrogen release by *Cyanothece* enabled *S. bacillaris* to become four times more abundant in the species mixture than it would have been in monoculture. This intricate interplay between competition and facilitation is likely to be a major determinant of the relative abundances of unicellular nitrogen-fixing cyanobacteria and non-nitrogen-fixing phytoplankton species in the oligotrophic ocean.

Primary production in many oceanic environments is often limited by the availability of nitrogen (Falkowski 1997; Capone 2000; Agawin et al. 2002). Sources of new

nitrogen therefore play an important role in the productivity of marine ecosystems. One of the sources of new nitrogen is biological nitrogen fixation, which provides a significant nitrogen input in marine ecosystems (Gruber and Sarmiento 1997; Karl et al. 1997; LaRoche and Breitbarth 2005). The large filamentous cyanobacterium *Trichodesmium* has long been recognized as one of the major nitrogen-fixing organisms in the tropical oceans (Capone et al. 1997; Sañudo-Wilhelmy et al. 2001). In addition, several species of small unicellular cyanobacteria are also capable of nitrogen fixation (Wyatt and Silvey 1969; Mitsui et al. 1986), and recent discoveries show that these can make important contributions to the oceanic nitrogen budget (Zehr et al. 2001; Montoya et al. 2004).

Although nitrogen-fixing cyanobacteria have access to a seemingly unlimited pool of nitrogen, they face competition from numerous, often faster growing, non-fixing phytoplankton species. A better understanding of these species interactions is essential to improve prediction of the ecological conditions favoring nitrogen-fixing organisms.

¹ Present address: Biology Department, Universidad de las Islas Baleares, E-07122 Palma de Mallorca, Spain.

² Corresponding author (jef.huisman@science.uva.nl).

Acknowledgments

We thank C. Sigon and H. Balke for their practical advice and support with the chemostat experiments, and L.J. Stal and two anonymous reviewers for their valuable comments on the manuscript.

N.S.R.A. gratefully acknowledges financial support from the Marie Curie Postdoctoral Fellowship Program (Contract HPMF-CT-2002-02135) of the European Commission and the Juan de la Cierva and Ramon y Cajal Program of the Spanish Ministry of Education and Science. The research of S.H. and J.H. was supported by the Earth and Life Sciences Foundation (ALW), which is subsidized by the Netherlands Organization for Scientific Research (NWO).

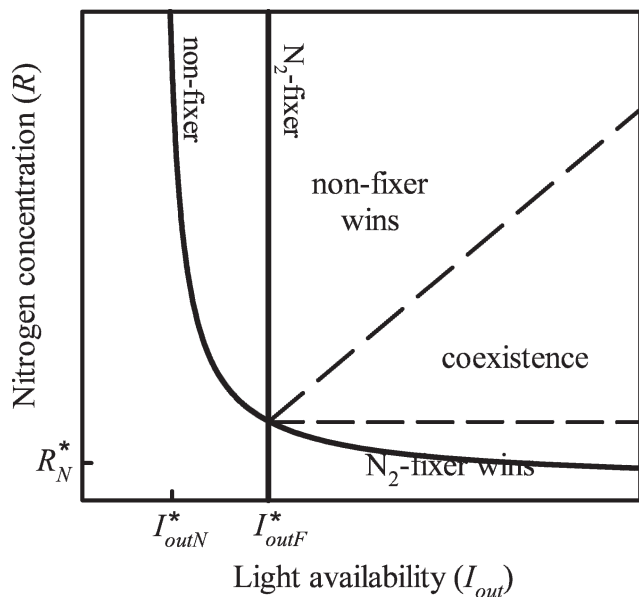


Fig. 1. A simple conceptual model of competition for nitrogen and light between a nitrogen-fixing cyanobacterium and a non-fixing phytoplankton species. Solid lines represent their zero isoclines. I_{outN}^* and I_{outF}^* indicate the critical light intensities of the non-fixer and the fixer, respectively, whereas R_N^* indicates the critical nitrogen requirements of the non-fixer. It is assumed that the nitrogen-fixing cyanobacterium does not require dissolved inorganic nitrogen. It is further assumed that the non-fixer is a better competitor for light. Hence, the zero isoclines of the two species intersect. The dashed diagonal line represents the slope of the consumption vector of the non-fixer, and the dashed horizontal line represents the slope of the consumption vector of the nitrogen fixer. In each region of the graph, the outcome of competition is indicated for supply points falling into that region.

During the past few decades, a firm body of theory has been developed to predict the population dynamics of phytoplankton species engaged in competition for nutrients (Tilman 1982; Grover 1997; Klausmeier et al. 2004) and competition for light (Huisman and Weissing 1994; Litchman and Klausmeier 2001; Stomp et al. 2004). Many of these competition models have been well tested in laboratory experiments with freshwater phytoplankton (Tilman 1977; Huisman et al. 1999; Passarge et al. 2006) and marine phytoplankton species (Sommer 1986, 1994; Stomp et al. 2004). Predictions on phytoplankton species composition, derived from this combination of theory and experiments, have been successfully applied to a variety of different field situations (Sommer 1993; Huisman et al. 2004; Stomp et al. 2007).

Similar competition models have been developed to study the interactions between nitrogen-fixing cyanobacteria and non-nitrogen-fixing phytoplankton (Smith 1983; Tyrrell 1999). The core of current thinking on competition between nitrogen-fixing cyanobacteria and other phytoplankton can be visualized using Tilman's (1982) graphical isocline approach (Fig. 1). Zero isoclines of species plot the critical threshold values of environmental conditions below which these species will have negative net growth rates (i.e., will disappear). Suppose, for instance, that two species

compete for nitrogen and light. We shall indicate the critical threshold value for dissolved inorganic nitrogen of a species by the symbol R^* , and the critical threshold value for light by the symbol I_{out}^* . Competition theory predicts that the species with the lowest critical nitrogen requirements (lowest R^*) will be the superior competitor for nitrogen (Tilman 1982), whereas the species with the lowest critical light intensity (lowest I_{out}^*) will be the superior competitor for light (Huisman and Weissing 1994).

Nitrogen-fixing cyanobacteria can grow on dinitrogen. Hence, the zero isocline of the nitrogen-fixing cyanobacterium can be drawn as a straight vertical line, independent of the concentration of dissolved inorganic nitrogen (Fig. 1). The zero isocline of the non-fixing phytoplankton species is bounded by its R^* and I_{out}^* values and can be drawn as a curved line, indicating that nitrogen and light limitation have interacting effects on phytoplankton growth (Rhee and Gotham 1981; Healey 1985). Given the high costs of nitrogen fixation, it seems plausible that non-fixing phytoplankton species generally have lower light requirements than nitrogen-fixing cyanobacteria and hence would be better competitors for light. As a result, the zero isoclines of the two species intersect (Fig. 1), indicating that they can coexist for suitable combinations of nitrogen and light supply. Finally, Fig. 1 assumes that the nitrogen-fixing cyanobacterium does not consume dissolved inorganic nitrogen, which guarantees that the coexistence equilibrium is stable. With this graphical configuration, competition theory predicts that the non-fixing species becomes dominant in systems with a high nitrogen supply, the nitrogen-fixing cyanobacterium becomes dominant at a low nitrogen supply, while the two species will coexist at a wide range of intermediate nitrogen inputs.

Competition experiments with N_2 -fixing cyanobacteria that would enable tests of this conceptual model have been scarce. Moreover, several aspects make competition between nitrogen fixers and non-nitrogen fixers more complicated, and hence more challenging, than suggested by this simple conceptual model. First, several nitrogen-fixing cyanobacteria can also consume ammonium, and sometimes nitrate, and switch to nitrogen fixation only when the availability of these other nitrogen sources is reduced (e.g., Zevenboom et al. 1981; Mulholland et al. 2001; Holl and Montoya 2005). Hence, nitrogen-fixing cyanobacteria can compete for dissolved inorganic nitrogen with non-fixing species. Second, nitrogen fixation is energetically quite expensive and therefore often depends on the light conditions (Staal et al. 2002; Rabouille et al. 2006). Therefore, the zero isoclines of nitrogen-fixing species will not be straight vertical lines. Third, nitrogen fixers can excrete fixed nitrogen (Capone et al. 1994; Mulholland and Bernhardt 2005) and may thereby facilitate growth of non-fixing species (Karl et al. 1995; Mulholland et al. 2006). This would affect the coexistence region in Fig. 1. Accordingly, each of these three considerations adds further complexity to the simple conceptual model of Fig. 1.

In this article, we develop new theory on the competition between nitrogen-fixing and non-nitrogen-fixing phytoplankton that incorporates the complicating processes just

mentioned. We then use monoculture experiments to estimate the model parameters of three marine phytoplankton species. Finally, we test the model predictions in a series of competition experiments, using small unicellular nitrogen-fixing cyanobacteria in competition against non-nitrogen-fixing phytoplankton.

Theory

Competition model—Our model is an extension of earlier competition models developed by Tilman (1982), Huisman and Weissing (1995), Boushaba and Pascual (2005), and Passarge et al. (2006). We consider a well-mixed water column, with a limited amount of inorganic nitrogen, a nitrogen-fixing cyanobacterium, and a non-nitrogen-fixing phytoplankton species. Let P_F denote the population density (cells per unit volume) of the nitrogen-fixing cyanobacterium, P_N the population density of the non-nitrogen-fixer, and R the concentration of dissolved inorganic nitrogen (molar concentrations). We assume that the nitrogen fixer can consume both nitrate and dinitrogen. Furthermore, we assume that part of the nitrogen fixed by the nitrogen fixer is excreted and thereby adds new nitrogen to the available nitrogen pool. The population dynamics of the two species can be written as a balance between growth processes and losses (e.g., mortality):

$$\frac{dP_N}{dt} = \overline{g_N}P_N - m_N P_N \quad (1)$$

$$\frac{dP_F}{dt} = (\overline{g_{FNO_3}} + \overline{g_{FN_2}})P_F - m_F P_F \quad (2)$$

$$\begin{aligned} \frac{dR}{dt} = & D(R_{in} - R) - Q_N \overline{g_N} P_N \\ & - Q_F \overline{g_{FNO_3}} P_F + \varepsilon_F Q_F \overline{g_{FN_2}} P_F \end{aligned} \quad (3)$$

Equation 1 describes the growth and losses of the non-nitrogen fixer, where g_N is its specific growth rate (h^{-1}) and m_N is its specific loss rate (h^{-1}). Equation 2 describes the growth and losses of the nitrogen-fixing cyanobacterium, where g_{FNO_3} and g_{FN_2} represent its specific growth rate based on nitrate uptake and on N_2 fixation, respectively, and m_F is its specific loss rate. The horizontal bars indicate that the growth rates are depth-averaged. Equation 3 describes the dynamics of the concentration of dissolved inorganic nitrogen, where D is the rate constant of nitrogen supply (e.g., by mineralization; h^{-1}), and R_{in} indicates the magnitude of the nitrogen supply (molar concentrations). In a chemostat, D would represent the dilution rate, which determines both the rate of nutrient supply and the loss rates of the species (i.e., $m_N = m_F = D$), and R_{in} would be the nitrogen input concentration of the mineral medium supplied to the chemostat. The second and third term in Eq. 3 describe the consumption of dissolved inorganic nitrogen by the two species, where Q_N and Q_F are the cellular nitrogen contents (also known as cell quotas; mol cell^{-1}) of the non-nitrogen fixer and nitrogen fixer,

respectively. Finally, the last term in Eq. 3 describes the excretion of nitrogen fixed by the nitrogen fixer, where ε_F is a dimensionless parameter indicating the magnitude of nitrogen excretion. We note, from Eqs. 2 and 3, that the fraction of the total nitrogen fixation that is excreted by the nitrogen fixer can be calculated as $\varepsilon_F/(1 + \varepsilon_F)$.

Specific growth rate of the non-fixer—The model assumes that nitrate availability, R , and light intensity, I ($\mu\text{mol photons m}^{-2} \text{s}^{-1}$), have interactive effects on the specific growth rate of the non-nitrogen fixer (Rhee and Gotham 1981; Healey 1985). This can be described by a multiplicative function of two Monod equations (Huisman and Weissing 1995):

$$g_N(R, I) = g_{maxN} \left(\frac{R}{M_N + R} \right) \left(\frac{I}{H_N + I} \right) \quad (4)$$

Here, g_{maxN} is the maximum specific growth rate (h^{-1}) of the non-nitrogen fixer, M_N is its half-saturation constant for nitrogen-limited growth (molar concentrations), and H_N is its half-saturation constant for light-limited growth ($\mu\text{mol photons m}^{-2} \text{s}^{-1}$).

Specific growth rate of the nitrogen fixer—We describe the specific growth rate of the nitrogen fixer by two components to account for its ability to grow on both N_2 (g_{FN_2}) and nitrate (g_{FNO_3}). Several nitrogen-fixing organisms first consume nitrate before they invest in the energetically more expensive fixation of dinitrogen. As a result, the activity of nitrogen fixation is often sensitive to the concentration of nitrate (Mulholland et al. 2001; Holl and Montoya 2005). Similar to more detailed physiological models of the nitrogen fixation process, we therefore assume that the nitrogen fixation rate takes its maximum value in absence of nitrate, decreases with nitrate availability, and increases with light availability (Rabouille et al. 2006). Accordingly, we model the specific growth rate due to nitrogen fixation by the following formulation:

$$g_{FN_2}(R, I) = g_{maxFN_2} \left(\frac{M_{FN_2}}{M_{FN_2} + R} \right) \left(\frac{I}{H_{FN_2} + I} \right) \quad (5)$$

where g_{maxFN_2} is the maximum specific growth rate under nitrogen-fixing conditions, M_{FN_2} is the half-saturation constant describing the decrease of the nitrogen fixation rate with increasing nitrate availability, and H_{FN_2} is the half-saturation constant for light-limited growth under nitrogen-fixing conditions. Analogous to the specific growth rate of the non-nitrogen fixer (Eq. 4), the model assumes that the specific growth rate due to nitrate assimilation by the nitrogen fixer is a multiplicative function of nitrate and light availability:

$$g_{FNO_3}(R, I) = g_{maxFNO_3} \left(\frac{R}{M_{FNO_3} + R} \right) \left(\frac{I}{H_{FNO_3} + I} \right) \quad (6)$$

where g_{maxFNO_3} is the maximum specific growth rate of the nitrogen-fixer during nitrate assimilation, M_{FNO_3} is its half-saturation constant for nitrogen-limited growth during

nitrate assimilation, and H_{FNO_3} is its half-saturation constant for light-limited growth during nitrate assimilation. To simplify the model, and to reduce the number of parameters, we assume that the half-saturation constants of nitrogen fixation and nitrate assimilation are similar ($M_F = M_{FN2} = M_{FNO_3}$). This implies that the increase of nitrate assimilation with nitrate availability is mirrored by a similar decrease of nitrogen fixation with nitrate availability. We further simplify the model by assuming that the half-saturation constants of light-limited growth under nitrogen fixation and under nitrate assimilation are similar; that is, $H_F = H_{FN2} = H_{FNO_3}$.

Incorporation of the light gradient—Light intensity decreases with depth, as photons are absorbed by, e.g., water, dissolved organic matter, and the phytoplankton species in the water column. Vertical positions within the water column will be indicated by the depth, z (m), which runs from $z = 0$ at the water surface to $z = z_M$ at the bottom of the surface-mixed layer. According to Lambert-Beer's law, the vertical light gradient can then be described as

$$I(z) = I_{in} \exp(-K_{bg}z - k_N P_N z - k_F P_F z) \quad (7)$$

where I_{in} is the incident light intensity at the water surface ($\mu\text{mol photons m}^{-2} \text{s}^{-1}$), K_{bg} is the background turbidity caused by water and dissolved organic matter (m^{-1}), and k_N and k_F are the specific light attenuation coefficients ($\text{m}^2 \text{cell}^{-1}$) of the non-nitrogen fixer and nitrogen fixer, respectively. For notational convenience, we define the light intensity transmitted to the bottom of the surface mixed layer as $I_{out} = I(z_M)$. We note from Eq. 7 that the light gradient is dynamic. That is, light transmission to the bottom of the mixed layer (I_{out}) will decrease with increasing phytoplankton population densities because of shading.

The depth-averaged specific growth rate of each species is obtained by integrating its local specific growth rate over depth as follows:

$$\bar{g}_i = \frac{1}{z_M} \int_0^{z_M} g_i(R, I(z)) dz, \quad i = N, FNO_3, FN2 \quad (8)$$

Using the Monod equation and Lambert-Beer's law, the depth integral in Eq. 8 can be solved. More precisely, an explicit equation for the depth-averaged specific growth rate of the non-nitrogen fixer can be derived by substitution of Eq. 4 and Eq. 7 into Eq. 8 and subsequent integration (Huisman and Weissing 1994, 1995):

$$\bar{g}_N = g_{maxN} \left(\frac{R}{M_N + R} \right) \times \left(\frac{\ln(H_N + I_{in}) - \ln(H_N + I_{out})}{\ln(I_{in}) - \ln(I_{out})} \right) \quad (9)$$

Similarly, by combining Eq. 5 and Eq. 6, the depth-averaged specific growth rate of the nitrogen fixer can be

written as

$$\bar{g}_F = \bar{g}_{FN2} + \bar{g}_{FNO_3} = \left(\frac{g_{maxFN2} M_F + g_{maxFNO_3} R}{M_F + R} \right) \times \left(\frac{\ln(H_F + I_{in}) - \ln(H_F + I_{out})}{\ln(I_{in}) - \ln(I_{out})} \right) \quad (10)$$

We note from this equation that the maximum specific growth rate of the nitrogen fixer equals g_{maxFN2} in the absence of nitrate, whereas it equals g_{maxFNO_3} in the presence of saturating concentrations of nitrate.

The full dynamical system is obtained by substituting Eq. 9 and Eq. 10 into Eqs. 1–3 in combination with Eq. 7 to describe changes in light transmission I_{out} . The model simulations were run using a fourth-order Runge-Kutta method.

This model predicts that each species has its own critical light intensity, called I_{out}^* (Huisman and Weissing 1994). The critical light intensity of a species can be measured under light-limited conditions and is defined as the light intensity measured at the bottom of a well-mixed water column at which the species can just maintain a stationary population ($dP_i/dt = 0$). Suppose, for instance, that all nutrients are available in ample supply and the population densities of the phytoplankton species increase. Then, light transmission through the water column will decline, and, thereby, the depth-averaged specific growth rates of the species will gradually diminish. Once light transmission is reduced below the critical light intensity of a species (i.e., $I_{out} < I_{out}^*$), this species will start to decline. This process will continue until, in the end, the species with the lowest critical light intensity has competitively displaced all other species. Accordingly, the model predicts that the species with the lowest critical light intensity will be the superior competitor for light (Huisman and Weissing 1994; Huisman et al. 1999). Likewise, each species has its own critical nitrogen requirements (R^*), and the model predicts that the species with the lowest critical nitrogen requirements will be the superior competitor under nitrogen-limited conditions (Tilman 1982).

Methods

Species—The experiments were performed with three marine phytoplankton species. The nitrogen fixer was represented by *Cyanothece* sp. Miami BG 043511 (formerly called *Synechococcus*; see Waterbury and Rippka 1989), which is a unicellular cyanobacterium capable of aerobic nitrogen fixation (Mitsui et al. 1986; Ikemoto and Mitsui 1994). The non-nitrogen fixers were represented by the cyanobacterium *Synechococcus bacillaris* CCMP 1333 and the marine green alga *Chlorella* cf. sp. CCMP 1227. All three unicellular species have been isolated from open ocean waters and grow optimally at temperatures of 22–26°C (<http://ccmp.bigelow.org>; Campbell et al. 1994). Cultures of the species have a green (*Chlorella*) or blue-green color (*Cyanothece* and *Synechococcus*), indicating that the species will compete for the same regions in the light spectrum (cf. Stomp et al. 2004). Both cyanobacteria

Table 1. System parameters and initial conditions used in the monoculture and competition experiments: incident light intensity (I_{in}), nitrate concentration in the inflowing mineral medium (R_{in}), background turbidity (K_{bg}), and the population densities of the species at the onset of the experiments. All experiments used a mixing depth of $z_M = 0.05$ m and a dilution rate of $D = 0.014$ h⁻¹.

Experiment	I_{in} ($\mu\text{mol m}^{-2} \text{s}^{-1}$)	R_{in} (mmol L ⁻¹)	K_{bg} (m ⁻¹)	Initial population density (million cells mL ⁻¹)		
				<i>Chlorella</i>	<i>Synechococcus</i>	<i>Cyanothece</i>
Monocultures						
<i>Chlorella</i>	40	0.1	4.75	0.50	0	0
<i>Chlorella</i>	40	8	4.75	2.5	0	0
<i>Synechococcus</i>	20	0.5	4.75	0	38.4	0
<i>Synechococcus</i>	20	1	4.75	0	8.9	0
<i>Synechococcus</i>	20	8	4.75	0	19.0	0
<i>Cyanothece</i>	20	0	11	0	0	0.60
<i>Cyanothece</i>	20	0.5	4.75	0	0	2.0
<i>Cyanothece</i>	20	8	4.75	0	0	12
<i>Cyanothece</i>	40	0	11	0	0	0.40
<i>Cyanothece</i>	40	0.1	11	0	0	0.80
<i>Cyanothece</i>	40	8	4.75	0	0	4.0
Competition						
<i>Cyanothece</i> × <i>Chlorella</i>	40	0.1	11	0.039	0	0.16
<i>Cyanothece</i> × <i>Chlorella</i>	40	8	4.75	0.060	0	0.50
<i>Cyanothece</i> × <i>Synechococcus</i>	20	0.1	4.75	0	5.0	1.2
<i>Cyanothece</i> × <i>Synechococcus</i>	20	0.5	4.75	0	5.5	0.25
<i>Cyanothece</i> × <i>Synechococcus</i>	20	1	4.75	0	14	0.20
<i>Cyanothece</i> × <i>Synechococcus</i>	20	8	4.75	0	7.0	0.075

contain phycocyanin as their predominant phycobilipigment, although they also contain minor amounts of phycoerythrin. *Cyanothece* sp. and *Chlorella* sp. both have an average cell diameter of ~5 μm , but can be distinguished on the basis of their pigment composition. *S. bacillaris* is a bacillus-like picocyanobacterium with an average cell diameter of only ~1 μm ; it was selected because we expected that its small size might make it a good competitor for light and nutrients and therefore an interesting organism to test the model predictions. Pilot experiments (data not shown) showed that all three species could grow well in our chemostats and mineral medium. The species were not grown axenically, but regular inspection with the microscope during the experiments showed that contamination with heterotrophic bacteria was always low, usually <1% of the total biovolume.

Chemostat experiments—The species were grown in laboratory-built chemostats specifically developed for the study of light-limited phytoplankton (Huisman et al. 1999). Each chemostat consisted of a flat culture vessel illuminated from one side to create a unidirectional light gradient. The culture vessels had inner dimensions of 27-cm height, 18-cm width, and an optical path length (“mixing depth”) of $z_M = 5$ cm. The effective working volume of the vessels was 1,600 mL. A water jacket placed between the light source and the culture vessel maintained the temperature of the culture vessel at 23°C. Homogeneous mixing and a sufficient supply of carbon dioxide (CO₂) and dinitrogen (N₂) were ensured by aerating the culture vessel with compressed air at a rate of 100–150 L h⁻¹. Before inoculation with phytoplankton, the culture vessels were heat sterilized for 1 h at 121°C. Nutrient medium was pumped from 3-liter bottles into the culture vessel by a peristaltic

pump (Watson Marlow 101U/R MkII) set at a dilution rate of $D = 0.014$ h⁻¹ (= 0.34 d⁻¹). An outlet enabled the outflow of the medium, together with the cultured phytoplankton.

We used these chemostats to run monoculture and competition experiments. The experimental settings of the chemostat experiments are given in Table 1. Monoculture experiments were used to estimate the parameter values of the species under different nitrogen-limited and light-limited conditions. From the parameter estimates thus obtained, we predicted the dynamics and outcome of competition for nitrogen and light. Finally, we tested these model predictions in competition experiments at different nitrogen and light levels.

Light—Light intensities (photosynthetically available radiation [PAR] from 400 to 700 nm, $\mu\text{mol photons m}^{-2} \text{s}^{-1}$) were measured with a Licor LI-189 quantum sensor attached to a LI-250 light meter (LI-COR). Light was supplied continuously by white fluorescent tubes (Philips PLL 24W/840/4P) placed in front of the culture vessel. The incident light intensity (I_{in}) was set by neutral density filters inserted between the light source and the front surface of the culture vessel. The light intensity penetrating through the cultures (I_{out}) was measured as the light intensity leaving the culture vessel at the back surface. To account for spatial variation, both I_{in} and I_{out} were measured at 10 regularly spaced positions at the front and back surface of the vessel, respectively. *Synechococcus* exhibited photoinhibition when grown at light intensities ≥ 40 $\mu\text{mol photons m}^{-2} \text{s}^{-1}$. Therefore the incident light intensity in the monoculture experiments and competition experiments with *Synechococcus* was set at $I_{in} = 20$ $\mu\text{mol photons m}^{-2} \text{s}^{-1}$. In the other experiments, the incident

light intensity was set at either $I_{in} = 20$ or $I_{in} = 40 \mu\text{mol photons m}^{-2} \text{s}^{-1}$ (Table 1). Critical light intensities (I_{out}^*) of the species were determined in monoculture experiments with a high nitrate input, as the average values of I_{out} when these light-limited monocultures had reached steady state.

Nitrogen—Cultures were grown on a mineral medium for marine nitrogen-fixing cyanobacteria, as described by Mitsui and Cao (1988). Sodium chloride (NaCl) was added to adjust the salinity to 30, and sodium hydroxide (NaOH) was added to adjust the pH to 8.5. The mineral medium contained an ample supply of all nutrients, except nitrogen. We added sodium nitrate (NaNO_3) to the medium as an inorganic nitrogen source. Nitrogen input concentrations that would generate a transition from nitrogen-limited to light-limited conditions in the ocean do not necessarily apply to laboratory chemostats. Therefore, we used simple scaling rules to estimate what nitrogen input concentrations and population densities would yield a transition from nitrogen limitation to light limitation at the laboratory scale. Under light-limited conditions, population density scales inversely proportional to the depth of the surface mixed layer (Petersen et al. 1997; Huisman 1999; Diehl et al. 2002). Our light-limited chemostats have a mixing depth of only 5 cm and can therefore produce population densities that are approximately three orders of magnitude higher than the population densities observed in a surface mixed layer of 50-m depth in the open ocean. High nitrogen input concentrations are required to sustain these high population densities. Based on a series of pilot experiments, we choose $R_{in} = 0 \text{ mmol L}^{-1}$ nitrate to induce nitrogen fixation in monocultures of *Cyanothece*, $R_{in} = 0.1 \text{ mmol L}^{-1}$ nitrate to create nitrogen-limited conditions for *Synechococcus* and *Chlorella*, and $R_{in} = 8 \text{ mmol L}^{-1}$ nitrate to induce light-limited conditions for all three species. In addition, we also ran chemostats with $R_{in} = 0.5$ and $R_{in} = 1 \text{ mmol L}^{-1}$ nitrate to induce conditions on the edge of nitrogen limitation and light limitation.

Concentrations of dissolved inorganic nitrogen (nitrate, nitrite, ammonium) in the cultures were determined once every 3 d in duplicate after filtration of 10-mL samples through glass fiber filters (Whatman GF/F, $0.7 \mu\text{m}$). Dissolved inorganic nitrogen was analyzed using a Technicon TRAACS 800 rapid flow autoanalyzer. Ammonium was detected as indo-phenolblue-complex at 630 nm (Helder and de Vries 1979). Nitrate was reduced in a copper cadmium coil to nitrite, using imidazole as a buffer, and then measured as nitrite. Nitrite was measured by diazotization with sulfanilamide and N-(1-naphtyl)-ethylene diammonium-dichloride to form a pink dye measured at 550 nm (Grasshoff 1967). All measurements were calibrated with standards diluted in low nutrient seawater. Detection limits were $0.05 \mu\text{mol L}^{-1}$ for nitrate, $0.03 \mu\text{mol L}^{-1}$ for nitrite, and $0.02 \mu\text{mol L}^{-1}$ for ammonium. Critical nitrogen requirements (R^*) of the species were determined from the monoculture experiments with a low nitrate input, as the average values of dissolved inorganic nitrogen when these nitrogen-limited monocultures were in steady state.

Cellular nitrogen contents (Q) of the species were determined by filtering 10–20-mL samples of the monocultures onto Whatman GF/F filters previously combusted for 3 h at 450°C . The loaded filters were freeze-dried for conservation until analysis. Cellular nitrogen content was measured using a Fisons CN elemental analyzer.

Phytoplankton counts—Phytoplankton population densities of the monoculture and competition experiments were sampled almost every day. Triplicate 1.8-mL samples were fixed with 0.2 mL of 1% glutaraldehyde and vortexed for a couple of seconds. They were left standing at 4°C for 20 min, then frozen in liquid nitrogen. The samples were stored at -80°C until cell count analyses using a Coulter EPICS XL MCL flow cytometer (Beckman Coulter Nederland BV). The flow cytometer distinguished between the species based on differences in pigment composition and cell size (e.g., Jonker et al. 1995; Veldhuis and Kraay 2004; Stomp et al. 2004). The orange fluorescence of phycoerythrin was used to separate the two cyanobacterial species from the green alga *Chlorella*. The magnitude of the scattering signal and chlorophyll fluorescence successfully distinguished between the small *Synechococcus* cells and the larger cells of *Cyanothece* and *Chlorella*.

Parameter estimation—The model parameters were estimated from the experiments. For this purpose, it is useful to distinguish between system parameters and species parameters. System parameters are under experimental control. The preceding paragraphs already specified several of the system parameters, including the incident light intensity (I_{in}), the nitrogen concentration of the inflowing mineral medium (R_{in}), the dilution rate (D), and the optical path length (mixing depth) of the chemostats (z_M) (Table 1). The background turbidity (K_{bg}) was determined from measurements of I_{in} and I_{out} in chemostats filled with mineral medium but without phytoplankton. More precisely, according to Lambert-Beer's law (Eq. 7), the background turbidity can then be calculated as $K_{bg} = \ln(I_{in}/I_{out})/z_M$.

Species parameters describe the physiological features of each strain. They were estimated from the monoculture experiments. The cellular nitrogen contents (Q_i) of the species were determined from filtered samples, as described in one of the previous sections. The specific light extinction coefficients of the species were calculated from Lambert-Beers law. More precisely, for monocultures Eq. 7 can be written as

$$\ln(I_{in}/I_{out})/z_M = k_i P_i + K_{bg} \quad (11)$$

Accordingly, we monitored the population densities (P_i) and light transmission (I_{out}) during the monoculture experiments and then applied linear regression to the term $\ln(I_{in}/I_{out})/z_M$ plotted against P_i . The specific light extinction coefficient (k_i) was estimated as the slope of the linear regression.

The remaining species parameters are the maximum specific growth rates (g_{max}), the half-saturation constants

for nitrogen-limited growth (M) and light-limited growth (H), and nitrogen excretion by the nitrogen-fixing cyanobacterium (ε_F). Values for these parameters were estimated by model calibration. More precisely, we fitted time courses predicted by the model to the time courses of population density (P_i), light transmission (I_{out}), and nitrogen concentration (R) measured in the monoculture experiments (Huisman et al. 1999; Passarge et al. 2006). The model calibration was applied to all monoculture experiments of a species simultaneously, in one run, to estimate a unique set of parameter values for each species. For this purpose, measured data were first log-transformed to homogenize the variances. Subsequently, for each monoculture experiment the log-transformed values of population density, light transmission, and nutrient concentration were normalized, using the total sum of squares of each of these variables as a weighting factor. Parameter estimates were obtained by fitting the model predictions to these log-transformed normalized data by minimization of the residual sum of squares, using the Gauss-Marquardt-Levenberg algorithm. The model calibration was performed with the software package FEMME (Soetaert et al. 2002).

The species parameters that were estimated from the monoculture experiments were used to predict the population dynamics in the competition experiments.

Results

Monoculture experiments—

Chlorella: Figure 2 shows the time courses of the two monoculture experiments with the green alga *Chlorella*, both carried out at an incident light intensity of $I_{in} = 40 \mu\text{mol photons m}^{-2} \text{s}^{-1}$. In the first experiment, run with a low nitrate input concentration of $R_{in} = 0.1 \text{ mmol L}^{-1}$, population density increased and, hence, both the nitrate concentration and the light transmission through the culture decreased until a steady state was reached after 7 to 10 days (Fig. 2A). The steady state of this *Chlorella* culture was characterized by a population density of ~ 1.2 million cells mL^{-1} , a light transmission of $\sim 25 \mu\text{mol photons m}^{-2} \text{s}^{-1}$, and a dissolved inorganic nitrogen concentration of $\sim 1.39 \mu\text{mol L}^{-1}$ (Table 2). Because this experiment was run at a low nitrate input, the steady-state concentration of dissolved inorganic nitrogen reflects the R^* value for nitrogen of *Chlorella*. Thus, we obtained an estimate of $R^* = 1.39 \mu\text{mol nitrogen L}^{-1}$ for *Chlorella*.

The other monoculture experiment was run with a high nitrate input concentration of $R_{in} = 8 \text{ mmol L}^{-1}$ (Fig. 2B). Here, a much higher steady-state population density of ~ 2.6 million cells mL^{-1} was reached. Given the saturating nitrate concentrations, the steady-state light transmission reflects the I_{out}^* value of *Chlorella*. Thus, we estimated that $I_{out}^* = 14.7 \mu\text{mol photons m}^{-2} \text{s}^{-1}$ (Table 2). The species parameters obtained from these monoculture experiments are given in Table 3. The specific light extinction coefficient of *Chlorella* attained two distinctly different values: it was lower under nitrogen-limited conditions than under light-limited conditions. This indicates that *Chlorella* adjusted its

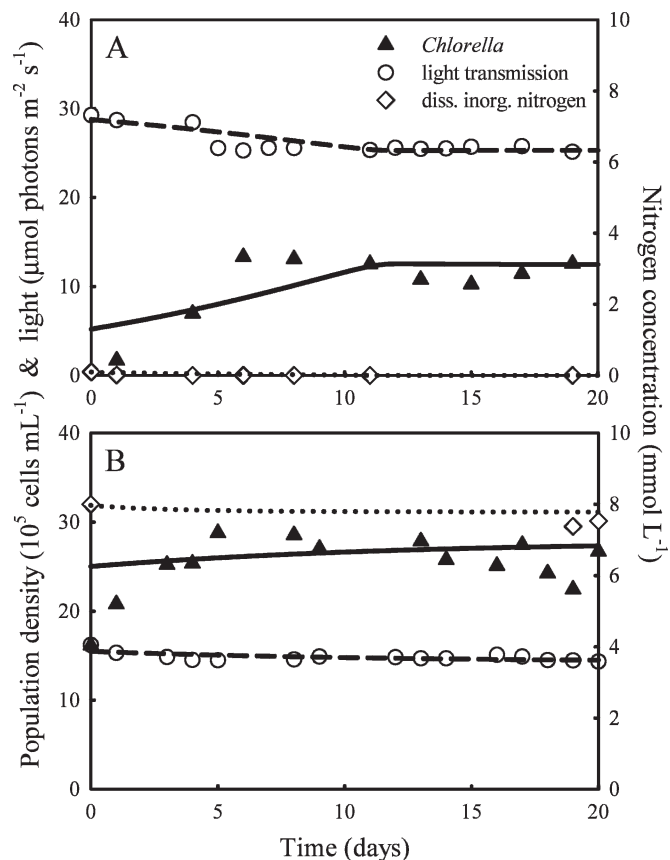


Fig. 2. Monoculture experiments of the green alga *Chlorella* CCMP 1227 at high light ($I_{in} = 40 \mu\text{mol photons m}^{-2} \text{s}^{-1}$), with (A) low nitrate input ($R_{in} = 0.1 \text{ mmol L}^{-1}$), and (B) high nitrate input ($R_{in} = 8 \text{ mmol L}^{-1}$). Symbols represent measurements of population density (triangles), light intensity I_{out} transmitted through the cultures (circles), and concentration of dissolved inorganic nitrogen (diamonds). Lines represent model predictions of population density (solid lines), transmitted light (dashed lines), and dissolved inorganic nitrogen (dotted lines). System parameters and initial conditions are given in Table 1, and parameter values of *Chlorella* are given in Table 3.

pigment content to the prevailing nitrogen and light conditions. The model predictions generally fit well to the monoculture experiments of *Chlorella* (compare symbols and lines in Fig. 2).

Synechococcus: Pilot experiments (not shown) indicated that the growth rate of the picocyanobacterium *Synechococcus* was inhibited at light intensities $\geq 40 \mu\text{mol photons m}^{-2} \text{s}^{-1}$. Therefore, the three monoculture experiments of *Synechococcus* were carried out at a low incident light intensity of $I_{in} = 20 \mu\text{mol photons m}^{-2} \text{s}^{-1}$. In all three experiments, *Synechococcus* reached high steady-state population densities of ~ 40 million cells mL^{-1} (Fig. 3). The large difference in steady-state population density between *Chlorella* and *Synechococcus* is mostly caused by a difference in cell size between the two species (cell diameters of $5 \mu\text{m}$ and $1 \mu\text{m}$, respectively).

The specific light extinction coefficient of *Synechococcus* (k_{Syne} , calculated by Eq. 11), was highly dynamic. It

Table 2. Steady-state characteristics of the monoculture experiments: incident light intensity (I_{in}), nitrate input concentration (R_{in}), population density, light transmission (I_{out}), and residual concentration of dissolved inorganic nitrogen (R ; including nitrate, nitrite, and ammonium). Standard deviation is shown in parentheses ($n = 3-10$, depending on the monoculture experiment).

Species	I_{in} ($\mu\text{mol m}^{-2} \text{s}^{-1}$)	R_{in} (mmol L $^{-1}$)	Population density (million cells mL $^{-1}$)	I_{out} ($\mu\text{mol m}^{-2} \text{s}^{-1}$)	I_{out}/I_{in} (%)	R ($\mu\text{mol L}^{-1}$)
<i>Chlorella</i>	40	0.1	1.18 (± 0.11)	25.5 (± 0.2)	63.8 (± 0.5)	1.39 (± 0.75)
<i>Chlorella</i>	40	8	2.64 (± 0.20)	14.7 (± 0.2)	36.7 (± 0.6)	7,455 (± 110)
<i>Synechococcus</i>	20	0.5	40.9 (± 0.1)	6.61 (± 0.57)	33.1 (± 2.9)	0.55 (± 0.05)
<i>Synechococcus</i>	20	1	39.6 (± 0.6)	3.86 (± 0.81)	19.3 (± 4.1)	456 (± 200)
<i>Synechococcus</i>	20	8	40.5 (± 0.2)	3.71 (± 0.21)	18.6 (± 1.1)	7,384 (± 43)
<i>Cyanothece</i>	20	0	2.03 (± 0.02)	7.01 (± 0.18)	35.1 (± 0.9)	1.80 (± 1.01)
<i>Cyanothece</i>	20	0.5	3.52 (± 0.12)	6.51 (± 0.07)	32.6 (± 0.4)	1.58 (± 0.82)
<i>Cyanothece</i>	20	8	4.45 (± 0.21)	4.65 (± 0.23)	23.3 (± 1.2)	7,744 (± 143)
<i>Cyanothece</i>	40	0	3.33 (± 0.13)	9.67 (± 0.16)	24.2 (± 0.4)	1.00 (± 0.24)
<i>Cyanothece</i>	40	0.1	3.91 (± 0.25)	7.25 (± 0.25)	18.1 (± 0.6)	0.74 (± 0.19)
<i>Cyanothece</i>	40	8	8.93 (± 0.69)	3.10 (± 0.08)	7.8 (± 0.2)	7,382 (± 49)

strongly increased with decreasing light availability (Fig. 4). This indicates rapid acclimation of the cellular pigment content of *Synechococcus* to the prevailing light conditions. The relationship was the same for all three monocultures, and could be described by the following equation (Fig. 4):

$$k_{\text{Syne}} = 1.37 - 0.50 \ln(I_{\text{out}}) \quad (12)$$

where k_{Syne} is expressed in $\mu\text{m}^2 \text{cell}^{-1}$. Pilot experiments (not shown) indicated that the specific light extinction coefficient of non-acclimated *Synechococcus* cells rapidly converged to Eq. 12. We therefore described the dynamics of this acclimation process as

$$\frac{dk_{\text{Syne}}}{dt} = \alpha(1.37 - 0.50 \ln(I_{\text{out}}) - k_{\text{Syne}}) \quad (13)$$

where α is the rate of acclimation, which was estimated to have a value of $\sim 3 \text{ h}^{-1}$. We note that Eq. 12 is the equilibrium solution of Eq. 13. Since changes in light

Table 3. Species parameters estimated from the monoculture experiments.

Symbol	<i>Chlorella</i>	<i>Synechococcus</i>	<i>Cyanothece</i>	Units
g_{maxN}	0.060	0.051	n.a.	h^{-1}
g_{maxFNO_3}	n.a.	n.a.	0.084	h^{-1}
g_{maxFN_2}	n.a.	n.a.	LL: 0.060 HL: 0.025	h^{-1}
m	0.014	0.014	0.014	h^{-1}
H	80.0	24.8	LL: 56.0 HL: 70.0	$\mu\text{mol photons m}^{-2} \text{s}^{-1}$
M	0.308	0.0799	1.00	$\mu\text{mol N L}^{-1}$
Q	0.079	0.012	0.092	pmol N cell^{-1}
k	LN: 3.52 HN: 5.68	*	4.86	$\mu\text{m}^2 \text{cell}^{-1}$
ε	n.a.	n.a.	8.0	—

Abbreviations: n.a., not applicable; LL, low light (20 $\mu\text{mol photons m}^{-2} \text{s}^{-1}$); HL, high light (40 $\mu\text{mol photons m}^{-2} \text{s}^{-1}$); LN, low nitrate input (0.1 mmol L $^{-1}$); HN, high nitrate input (8 mmol L $^{-1}$).

* The specific light extinction coefficient of *Synechococcus*, k_{Syne} , is not treated as a parameter, but as a variable; it increases with decreasing light availability according to Eq. 13.

extinction coefficients of species affect the model predictions, especially under light-limited conditions, Eq. 13 was added to the model equations. The model predictions fitted well to all three monoculture experiments of *Synechococcus* (Fig. 3).

From the monoculture experiment with a low nitrate input (Fig. 3A), we estimated $R^* = 0.55 \mu\text{mol nitrogen L}^{-1}$ for *Synechococcus* (Table 2). Likewise, from the monoculture experiment with a high nitrate input (Fig. 3C), we estimated $I_{\text{out}}^* = 3.7 \mu\text{mol photons m}^{-2} \text{s}^{-1}$ (Table 2). This indicates that *Synechococcus* is a very strong competitor for light.

Cyanothece: Monoculture experiments with the nitrogen-fixing cyanobacterium *Cyanothece* were carried out at both a low incident light intensity of $I_{in} = 20 \mu\text{mol photons m}^{-2} \text{s}^{-1}$ and a high incident light intensity of $I_{in} = 40 \mu\text{mol photons m}^{-2} \text{s}^{-1}$. Population densities of 2–3 million cells mL $^{-1}$ were reached in the two monoculture experiments without nitrate input (Fig. 5A,D), thus demonstrating that *Cyanothece* can sustain a population under nitrogen-fixing conditions. However, much higher population densities were reached in the two monocultures with a high nitrate input, with up to ~ 4.5 million cells mL $^{-1}$ at low I_{in} (Fig. 5C) and ~ 9 million cells mL $^{-1}$ at high I_{in} (Fig. 5F). This shows that *Cyanothece* can grow quite efficiently on nitrate as well.

In monocultures with a low nitrate input concentration of $R_{in} = 0.1 \text{ mmol L}^{-1}$ and $R_{in} = 0.5 \text{ mmol L}^{-1}$, *Cyanothece* was able to reduce the available dissolved inorganic nitrogen to very low concentrations of 0.74 $\mu\text{mol L}^{-1}$ and 1.58 $\mu\text{mol L}^{-1}$, respectively (Table 2). These values were of a similar magnitude as the R^* value measured in the nitrogen-limited monoculture of *Chlorella* and slightly exceeded the R^* value of *Synechococcus* (Table 2), indicating that *Cyanothece* should be able to compete for dissolved inorganic nitrogen quite effectively against non-nitrogen-fixing phytoplankton species. Strikingly, in the two *Cyanothece* monocultures without nitrate input, dissolved inorganic nitrogen was also found in low but detectable concentrations (1.00 $\mu\text{mol L}^{-1}$ and 1.80 $\mu\text{mol L}^{-1}$; Table 2). Again, these concentrations

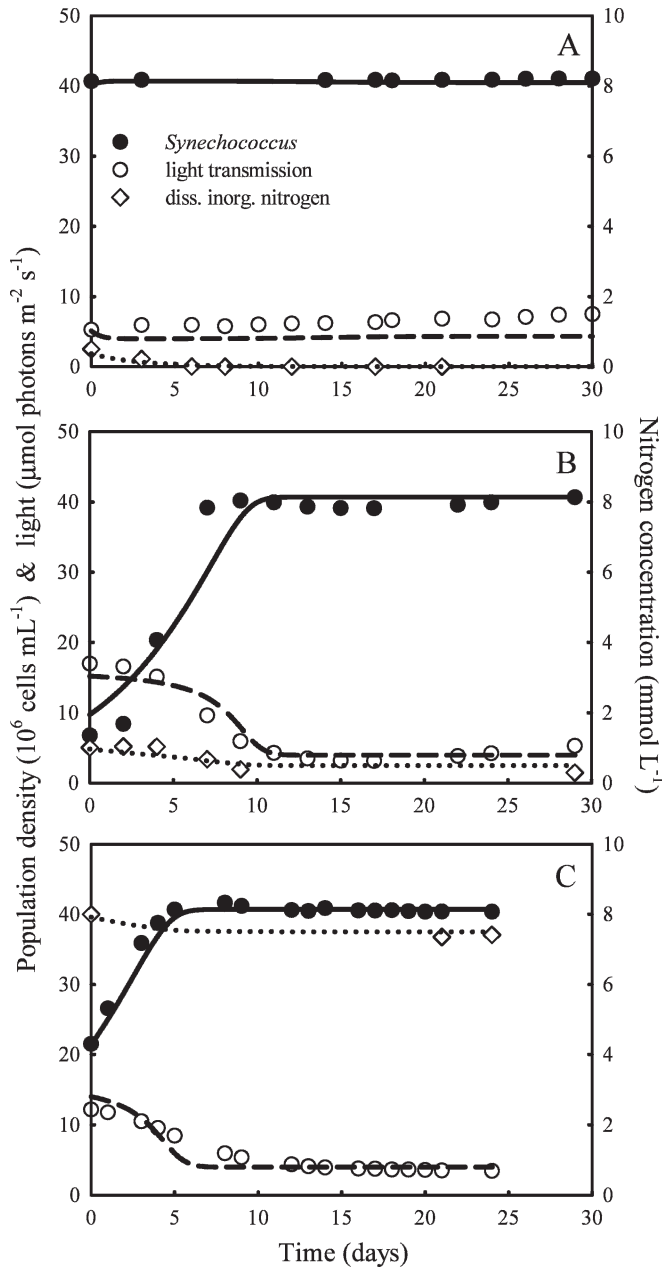


Fig. 3. Monoculture experiments of the picocyanobacterium *Synechococcus bacillaris* CCMP 1333 at low light ($I_{in} = 20 \mu\text{mol photons m}^{-2} \text{s}^{-1}$), with (A) low nitrate input ($R_{in} = 0.5 \text{ mmol L}^{-1}$), (B) intermediate nitrate input ($R_{in} = 1 \text{ mmol L}^{-1}$), and (C) high nitrate input ($R_{in} = 8 \text{ mmol L}^{-1}$). Symbols represent measurements of population density (closed circles), light intensity I_{out} transmitted through the cultures (open circles), and concentration of dissolved inorganic nitrogen (diamonds). Lines represent model predictions of population density (solid lines), transmitted light (dashed lines), and dissolved inorganic nitrogen (dotted lines). System parameters and initial conditions are given in Table 1, and parameter values of *Synechococcus* are given in Table 3.

exceeded the R^* value of *Synechococcus*. Furthermore, the model calibration indicated that *Cyanothece* excretes nitrogen, as the model calibration estimated a value of $\varepsilon_F = 8$ (Table 3). This suggests that *Cyanothece* is a rather

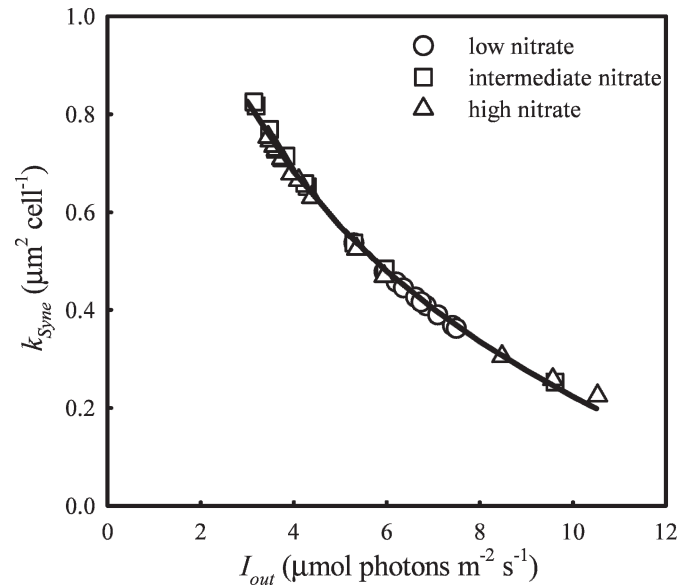


Fig. 4. The specific light extinction coefficient of the picocyanobacterium *Synechococcus*, k_{Syne} , decreases with increasing light availability. Symbols represent measurements of k_{Syne} in the monoculture experiments at low nitrate input ($R_{in} = 0.5 \text{ mmol L}^{-1}$; circles), intermediate nitrate input ($R_{in} = 1 \text{ mmol L}^{-1}$; squares), and high nitrate input ($R_{in} = 8 \text{ mmol L}^{-1}$; triangles). The line corresponds to Eq. 12 and was obtained by linear regression of k_{Syne} versus $\ln(I_{out})$ ($R^2 = 0.99$, $n = 34$, $p < 0.001$).

sloppy nitrogen fixer; apparently it first spills part of the nitrogen that it has fixed and thereafter consumes this spilled nitrogen again.

The specific light extinction coefficient, calculated by Eq. 11, maintained a constant value in *Cyanothece*, irrespective of the nitrogen and light conditions in the experiments (Table 3). Apparently, *Cyanothece* is less variable in its pigment content than *Chlorella* and *Synechococcus*. The monoculture experiments further showed that *Cyanothece* had a rather high critical light intensity of $I_{out}^* = 7\text{--}9.7 \mu\text{mol photons m}^{-2} \text{s}^{-1}$ in monocultures without nitrate, but a lower critical light intensity of $I_{out}^* = 3.1\text{--}4.7 \mu\text{mol photons m}^{-2} \text{s}^{-1}$ in monocultures with high nitrate input (Table 2). This indicates that *Cyanothece* is a relatively poor competitor for light under nitrogen-fixing conditions, whereas it is a strong competitor for light when it grows on nitrate. The model predictions generally fit well to the monoculture experiments of *Cyanothece* (Fig. 5).

Competition experiments—

Cyanothece versus *Chlorella*: In the first competition experiment between *Cyanothece* and *Chlorella*, with a low nitrate input the population densities of both species initially increased (Fig. 6A). As a result, the nitrate concentration and light transmission through the cultures declined. Competitive displacement started after ~ 10 d, when *Chlorella* started to decline. *Cyanothece* gradually approached a population density of ~ 4 million cells mL^{-1} ,

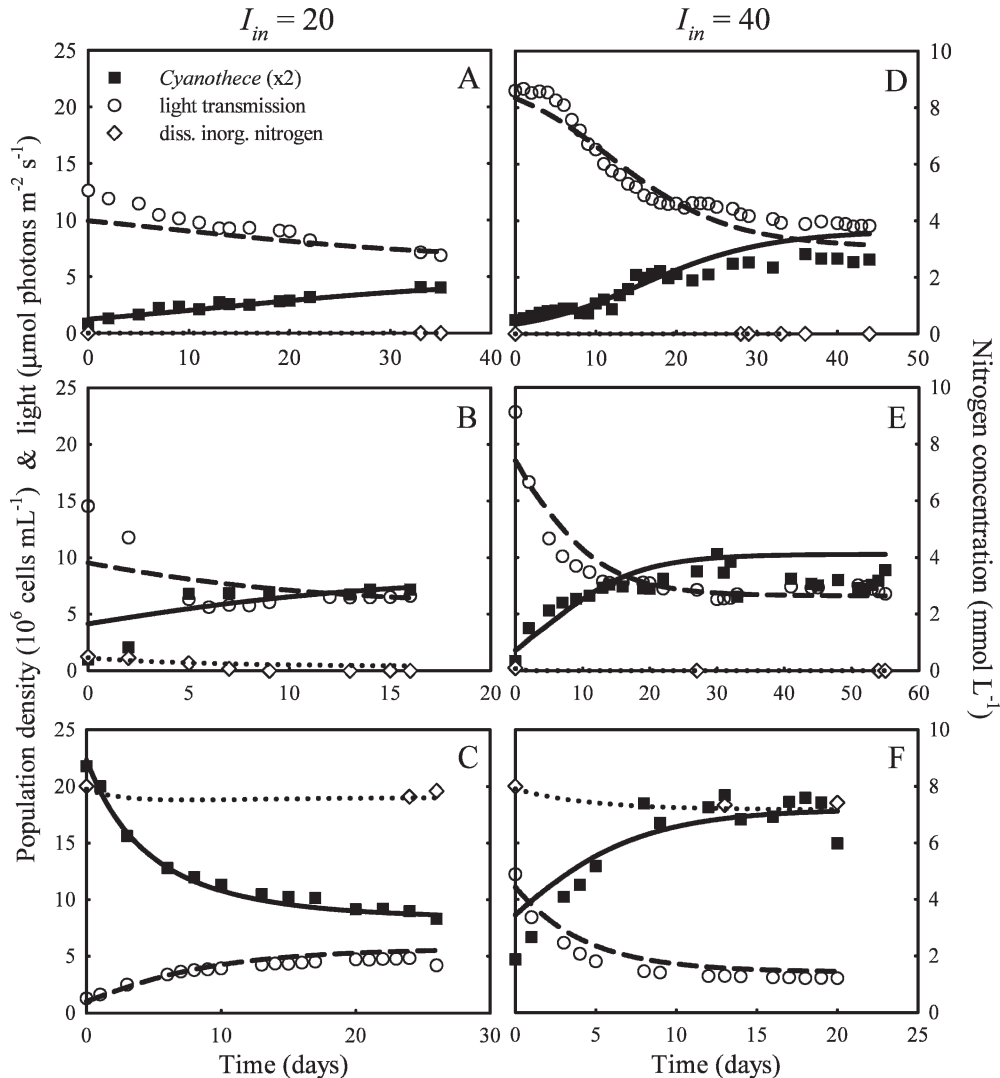


Fig. 5. Monoculture experiments of the nitrogen-fixing cyanobacterium *Cyanothece* at low light ($I_{in} = 20 \mu\text{mol m}^{-2} \text{s}^{-1}$), with (A) zero nitrate input ($R_{in} = 0 \text{ mmol L}^{-1}$), (B) intermediate nitrate input ($R_{in} = 0.5 \text{ mmol L}^{-1}$), and (C) high nitrate input ($R_{in} = 8 \text{ mmol L}^{-1}$). Monoculture experiments of *Cyanothece* at high light ($I_{in} = 40 \mu\text{mol m}^{-2} \text{s}^{-1}$), with (D) zero nitrate input ($R_{in} = 0 \text{ mmol L}^{-1}$), (E) low nitrate input ($R_{in} = 0.1 \text{ mmol L}^{-1}$), and (F) high nitrate input ($R_{in} = 8 \text{ mmol L}^{-1}$). Symbols represent measurements of population density (squares), light intensity I_{out} transmitted through the cultures (circles), and concentration of dissolved inorganic nitrogen (diamonds). Lines represent model predictions of population density (solid lines), transmitted light (dashed lines), and dissolved inorganic nitrogen (dotted lines). System parameters and initial conditions are given in Table 1, and parameter values of *Cyanothece* are given in Table 3. Note that the population density of *Cyanothece* is magnified by a factor two.

similar to its steady-state population density in monoculture under the same nitrate and light conditions (compare Fig. 6A with Fig. 5E), whereas *Chlorella* declined to a very low population density ($\sim 4\%$ of its steady-state population density in monoculture; compare Fig. 6A with Fig. 2A). In a similar fashion, *Cyanothece* competitively displaced *Chlorella* in the other competition experiment at a high nitrate input (Fig. 6B). The model predictions were in good agreement with the observed time courses of competition between *Cyanothece* and *Chlorella* (compare symbols and lines in Fig. 6).

Cyanothece versus *Synechococcus*: The competition experiment between *Cyanothece* and *Synechococcus* at the lowest nitrate input of $R_{in} = 0.1 \text{ mmol L}^{-1}$ is quite intriguing. The population densities of both species initially increased and, thereby, the light transmission through the cultures declined (Fig. 7A). After 12 days, competitive displacement started. *Synechococcus* increased to population densities of $\sim 35 \text{ million cells mL}^{-1}$ and thereby gradually displaced the nitrogen-fixing cyanobacterium *Cyanothece*. However, *Cyanothece* was not washed out. It remained present at population densities of $\sim 0.5 \text{ million}$

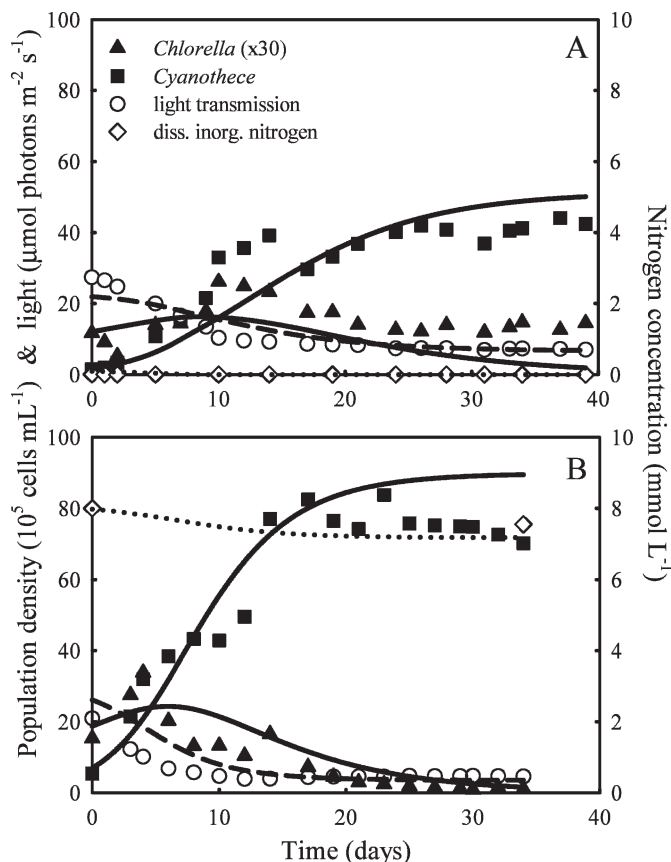


Fig. 6. Competition experiments between the green alga *Chlorella* and the nitrogen-fixing cyanobacterium *Cyanothecce* at high light ($I_m = 40 \mu\text{mol m}^{-2} \text{s}^{-1}$). *Cyanothecce* (squares) displaces *Chlorella* (triangles) at both (A) low nitrate input ($R_{in} = 0.1 \text{ mmol L}^{-1}$), and (B) high nitrate input ($R_{in} = 8 \text{ mmol L}^{-1}$). Circles indicate the light intensity I_{out} transmitted through the cultures, and diamonds indicate the concentration of dissolved inorganic nitrogen (the sum of nitrate, nitrite, and ammonium). Lines represent model predictions of population density (solid lines), transmitted light (dashed lines) and dissolved inorganic nitrogen (dotted lines). System parameters and initial conditions are given in Table 1, and parameter values of *Chlorella* and *Cyanothecce* are given in Table 3. Note that the population density of *Chlorella* is magnified by a factor 30.

cells mL^{-1} , which corresponds to $\sim 25\%$ of its monoculture population density under nitrogen-fixing conditions (compare Fig. 7A and Fig. 5A). Thus, *Cyanothecce* and *Synechococcus* coexist. This matches the model simulations, which predict that at this low nitrate input the two species approach stable coexistence through damped oscillations. The model simulations further revealed that *Synechococcus* could never have reached a population density of ~ 35 million cells mL^{-1} without the extra nitrogen provided by nitrogen-fixing *Cyanothecce* cells. More precisely, the model predicts that without *Cyanothecce* *Synechococcus* would have reached a lower steady-state population density of only ~ 8 million cells mL^{-1} under these culture conditions. This indicates that nitrogen fixation and subsequent nitrogen release by *Cyanothecce* was responsible for a four-fold higher abundance of *Synechococcus*.

The three other competition experiments, with a higher nitrate input, showed competitive exclusion (Fig. 7B–D). As predicted, *Synechococcus* was a stronger competitor for light and thereby displaced *Cyanothecce*. The rate of competitive displacement was faster at the two highest nitrate inputs (Fig. 7C,D) than at the relatively low nitrate input of $R_{in} = 0.5 \text{ mmol L}^{-1}$ (Fig. 7B).

Discussion

In this study, we developed a new competition model to predict the population dynamics of competition between nitrogen-fixing cyanobacteria and non-nitrogen-fixing phytoplankton species. We tested the model predictions in a series of dedicated chemostat experiments at different nitrate and light levels. During the various phases of model development, several complicating processes were incorporated, like the light dependence of nitrogen fixation, nitrate consumption by the nitrogen fixer, excretion of dissolved nitrogen by the nitrogen fixer, and pigment adaptation of *Synechococcus*. Additional model simulations (not shown) pointed out that the model was incapable of reproducing the experimental data if these processes had been ignored. Thus, the model structure greatly benefited from a tight interplay between theory and experiments.

Competition for light—The key findings of our study can be visualized graphically. Figure 8A plots the zero isoclines of the three investigated species, predicted by the model, as a function of the dissolved inorganic nitrogen concentration in the cultures (R) and light intensity transmitted through the cultures (I_{out}). The positions of the zero isoclines are consistent with the measurements of R and I_{out} in the steady-state monocultures (symbols in Fig. 8A). At high nitrate input concentrations, and when all other nutrients are also in ample supply, competition theory predicts that the species with the lowest critical light intensity (I_{out}^*) will be the superior competitor for light (Huisman and Weissing 1994; Huisman et al. 1999). Monoculture experiments showed that the critical light intensity of the picocyanobacterium *Synechococcus* was lower than that of the unicellular nitrogen-fixing cyanobacterium *Cyanothecce* (Table 2; at $I_m = 20$, $R_{in} = 8 \text{ mmol L}^{-1}$). The critical light intensity of *Cyanothecce*, in turn, was lower than that of the green alga *Chlorella* (Table 2; at $I_m = 40$, $R_{in} = 8 \text{ mmol L}^{-1}$). Hence, the critical light intensities of the three species can be ranked as

$$\begin{aligned} & \textit{Synechococcus} \text{ (CCMP 1333)} < \textit{Cyanothecce} \\ & < \textit{Chlorella} \text{ (CCMP 1227)} \end{aligned} \quad (14)$$

Competition experiments at high nitrate levels showed that *Synechococcus* displaced *Cyanothecce* (Fig. 7C,D), whereas *Cyanothecce* displaced *Chlorella* (Fig. 6B). Hence, in line with the model predictions, the species with the lowest critical light intensity was indeed the better competitor for light. Earlier competition studies using the same chemostat systems had shown that the picocyanobacterium *Synechocystis* PCC6803 was the best competitor for light among

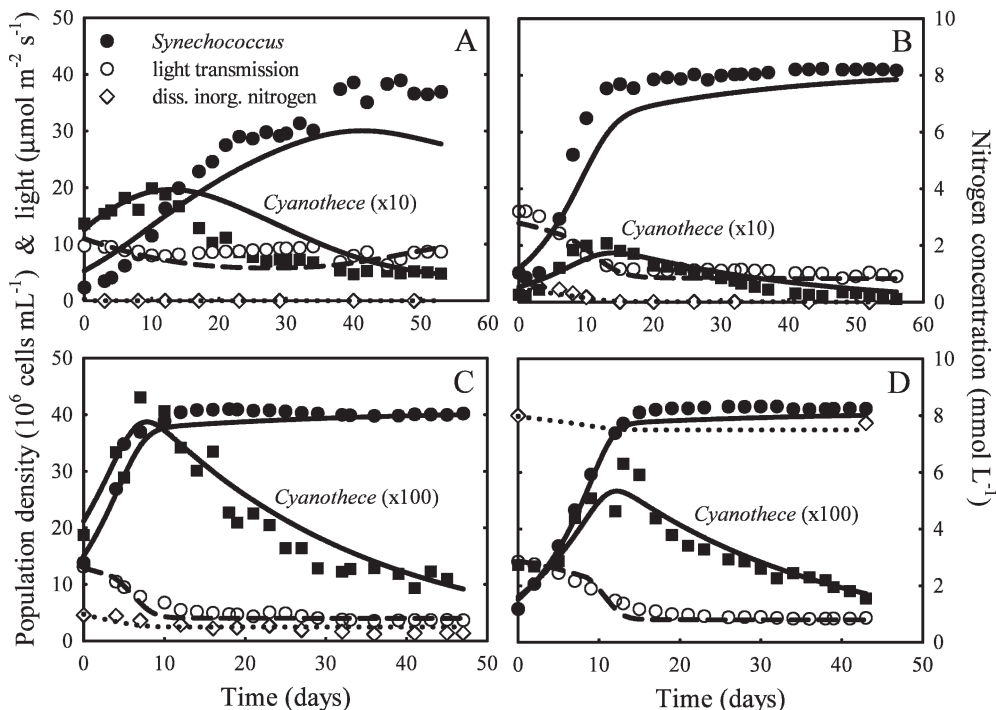


Fig. 7. Competition experiments between the picocyanobacterium *Synechococcus* and the nitrogen-fixing cyanobacterium *Cyanothece* at low light ($I_{in} = 20 \mu mol m^{-2} s^{-1}$). (A) *Synechococcus* (closed circles) and *Cyanothece* (squares) coexist at low nitrate input ($R_{in} = 0.1 mmol L^{-1}$). (B–D) *Synechococcus* (closed circles) displaces *Cyanothece* (squares) at (B) low-intermediate nitrate input ($R_{in} = 0.5 mmol L^{-1}$), (C) intermediate nitrate input ($R_{in} = 1 mmol L^{-1}$), and (D) high nitrate input ($R_{in} = 8 mmol L^{-1}$). Open circles indicate the light intensity I_{out} transmitted through the cultures, and diamonds indicate the concentration of dissolved inorganic nitrogen (the sum of nitrate, nitrite, and ammonium). Lines represent model predictions of population density (solid lines), transmitted light (dashed lines), and dissolved inorganic nitrogen (dotted lines). System parameters and initial conditions are given in Table 1, and parameter values of *Synechococcus* and *Cyanothece* are given in Table 3. Note that the population density of *Cyanothece* is magnified by a factor 10 in (A) and (B), and by a factor 100 in (C) and (D).

eight freshwater phytoplankton species (Huisman et al. 1999; Passarge et al. 2006). In total, these competition studies therefore confirm the general notion (e.g., Raven 1998) that picocyanobacteria, like *Synechocystis* and *Synechococcus*, are strong competitors for light as compared to larger phytoplankton species.

Interactions between nitrate and nitrogen fixation—Two different lines of evidence indicate that the nitrogen-fixing cyanobacterium *Cyanothece* could grow efficiently on nitrate. First, *Cyanothece* reached much higher population densities in nitrate-rich monoculture experiments than in nitrate-free experiments (compare Fig. 5F with Fig. 5D,E). Second, in monocultures with a low nitrate input, *Cyanothece* depleted the ambient nitrate concentration to $0.7\text{--}1.6 \mu mol L^{-1}$ (Table 2). This indicates that *Cyanothece* prefers nitrate assimilation as long as sufficient nitrate is available and switches to nitrogen fixation only if nitrate has been exhausted to the micromolar range. Strikingly similar findings have been reported for laboratory experiments with *Trichodesmium erythraeum* (strain IMS-101). Recent chemostat experiments showed that *Trichodesmium*

assimilated nitrate when supplied with sufficient nitrate, whereas it switched to nitrogen fixation when ambient nitrate concentrations was depleted to $0.3\text{--}0.4 \mu mol L^{-1}$ (Holl and Montoya 2005). This important feature, the switch from nitrate assimilation to nitrogen fixation when nitrate concentrations become low, was incorporated in our model (Eqs. 5 and 6).

From a physiological perspective, the energy requirements for nitrate assimilation are lower than for nitrogen fixation. Interestingly, and consistent with this physiological expectation, the critical light intensity of *Cyanothece* was lower in monocultures at high nitrate levels than in monocultures without nitrate (Table 2). As a consequence, the zero isocline of *Cyanothece* cannot be drawn as a straight vertical line, but bends off to higher light requirements at low nitrate levels (Fig. 8A). In other words, *Cyanothece* is a stronger competitor for light when grown on nitrate than when grown under nitrogen-fixing conditions.

Competition for nitrogen—At low nitrogen input concentrations, competition theory predicts that species will increase until the dissolved inorganic nitrogen is drawn to

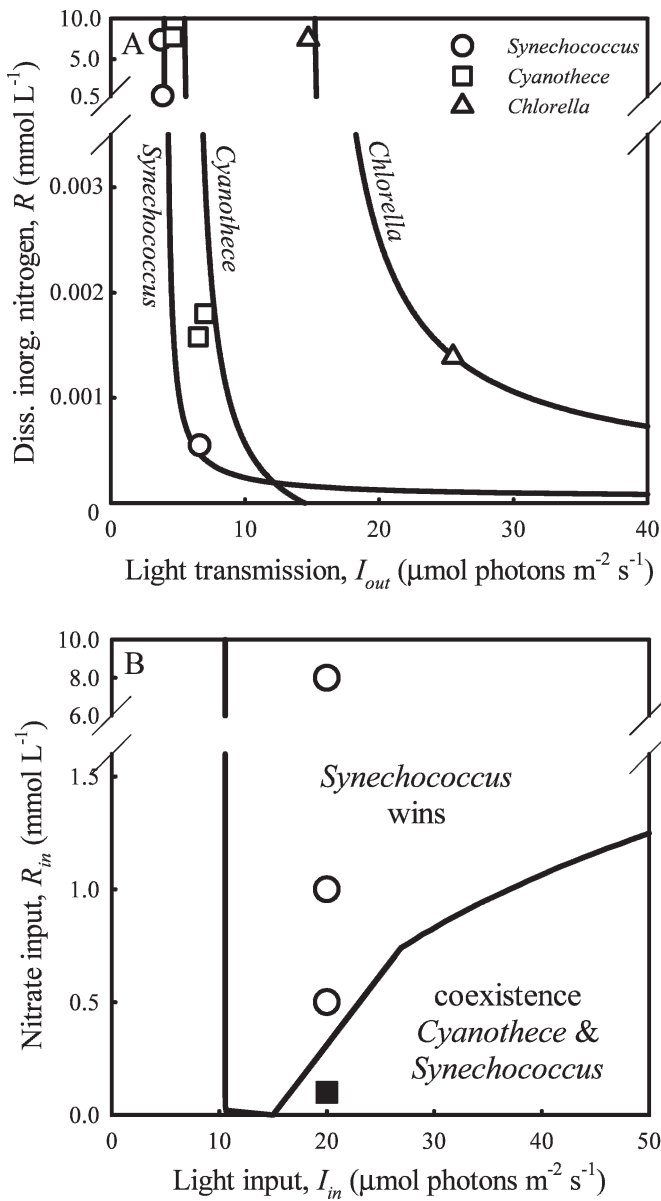


Fig. 8. (A) Zero isoclines of *Synechococcus*, *Cyanothece*, and *Chlorella* plotted as a function of light transmission (I_{out}) and concentration of dissolved inorganic nitrogen (R). The zero isoclines indicate the combinations of I_{out} and R at which the net growth rates of the species equal zero (i.e., $dP_i/dt = 0$). They are calculated by model simulations, assuming low light ($I_{in} = 20 \mu\text{mol m}^{-2} \text{s}^{-1}$) for *Synechococcus* and *Cyanothece*, and high light ($I_{in} = 40 \mu\text{mol m}^{-2} \text{s}^{-1}$) for *Chlorella*. Symbols represent the measured values of R and I_{out} at steady state in the monoculture experiments. (B) The outcome of competition between the picocyanobacterium *Synechococcus* and the nitrogen-fixing cyanobacterium *Cyanothece*, plotted as a function of incident light intensity (I_{in}) and nitrate input concentration (R_{in}). In each region of the graph, the outcome of competition is indicated for the combinations of I_{in} and R_{in} falling in that region. Symbols represent the locations of the competition experiments, where the square indicates the experiment that yielded stable coexistence, while the circles indicate the three experiments that led to competitive exclusion. The graph is based on $100 \times 500 = 50,000$ model simulations distributed on a grid of different I_{in} and

such a low concentration that none of the competing species can increase further. Hence, the species with the lowest critical nitrogen requirements (R^*) will be the superior competitor for nitrogen (Tilman 1982). Obviously, *Cyanothece* can grow without dissolved inorganic nitrogen, i.e., it has an R^* value of zero. The monoculture data show that *Synechococcus* has a lower R^* value than *Chlorella* (Table 2). The critical nitrogen requirements (R^*) of the species can therefore be ranked as:

$$\begin{aligned} & \textit{Cyanothece} < \textit{Synechococcus} \text{ (CCMP 1333)} \\ & < \textit{Chlorella} \text{ (CCMP 1227)} \end{aligned} \quad (15)$$

Equations 14 and 15 imply that, compared to *Synechococcus* and *Cyanothece*, *Chlorella* is a poor competitor under both light-limited and nitrogen-limited conditions, as also indicated by the position of its zero isocline (Fig. 8A). This was confirmed by the competition experiments, which showed that *Cyanothece* competitively displaced *Chlorella* (Fig. 6).

Coexistence by competition and facilitation—Further comparison of Eqs. 14 and 15 reveals that *Synechococcus* is a better competitor for light, whereas *Cyanothece* is a better competitor for nitrogen. That is, the zero isoclines of *Cyanothece* and *Synechococcus* intersect (Fig. 8A). This indicates that *Synechococcus* and *Cyanothece* may coexist when provided with suitable nutrient and light conditions. In the competition experiments with an intermediate to high nitrate input, *Synechococcus* was able to reduce light availability below the minimal light requirements of *Cyanothece*. Hence, *Synechococcus* displaced *Cyanothece* (Fig. 7B–D). In the competition experiment with the lowest nitrate input, however, the growth of *Synechococcus* became nitrogen limited, and therefore *Synechococcus* could not develop sufficient biomass to reduce light availability below the minimal light requirements of *Cyanothece*. Here, *Cyanothece* maintained a population, and the two species coexisted for the entire duration of the experiment (Fig. 7A). Earlier competition experiments with freshwater phytoplankton species, using phosphorus as a limiting nutrient, were unable to demonstrate species coexistence on the transition from nutrient to light limitation (Passarge et al. 2006). Hence, to the best of our knowledge, this experiment with *Synechococcus* and *Cyanothece* provides the first experimental demonstration of species coexistence mediated by competition for nutrients and light.

What is the mechanism of coexistence in this experiment? Clearly, *Synechococcus* was unable to exclude *Cyanothece*, because the population abundance of *Synechococcus* was nitrogen limited. However, if *Cyanothece* is capable to

←

R_{in} values; the simulations used the same mixing depth, dilution rate, and background turbidity as in the competition experiments (Table 1). Note the differences in scale between (A) and (B).

deplete dissolved inorganic nitrogen to very low concentrations and fix dinitrogen, why does *Cyanothece* not exclude *Synechococcus*? The model calibration pointed at a nitrogen excretion parameter of $\varepsilon_F = 8$ (Table 3). In view of Eqs. 2 and 3, this implies that of every nine molecules of nitrogen fixed by *Cyanothece*, eight molecules are released. In other words, *Cyanothece* might excrete 89% of its recently fixed nitrogen into the environment. This indicates that nitrogen release plays a quantitatively very important role, consistent with field studies of other nitrogen-fixing cyanobacteria (Gallon et al. 2002; Mulholland 2007; Ohlendieck et al. 2007). In fact, the high rate of nitrogen release by *Cyanothece* is of a similar magnitude as the nitrogen release of 70–90% recently estimated for chemostat cultures of the nitrogen-fixing cyanobacterium *Trichodesmium* IMS101 (e.g., Mulholland and Bernhardt 2005). *Synechococcus* can benefit from the nitrogen released by *Cyanothece*. More precisely, in the monoculture experiments without nitrate input, nitrogen release by *Cyanothece* raised the concentration of dissolved inorganic nitrogen above the critical nitrogen requirements (R^*) of *Synechococcus*. Hence, *Synechococcus* can invade a nitrogen-fixing *Cyanothece* population. According to our model simulations, this is indeed the mechanism that enabled the coexistence of the two species in this experiment. Even stronger, the model simulations indicated that *Synechococcus* reached a population density that, because of the nitrogen release by *Cyanothece*, was four times higher than its corresponding population density in monoculture. Thus, at low nitrate levels, the species interaction between *Cyanothece* and *Synechococcus* is transformed from competition into facilitation.

We exploited our parameterized model to obtain a better understanding of the region in parameter space that allowed coexistence of the two species. For this purpose, we ran 50,000 simulations in a fine grid with 100 different values of incident light intensity (I_{in}) and 500 nitrate input concentrations (R_{in}). All other parameters remained constant. Each of the simulations was run until a steady state was reached. Results are presented in Fig. 8B. Note that Fig. 8A plots the zero isoclines as a function of the residual resource concentrations (I_{out} , R), whereas Fig. 8B plots the outcome of competition as a function of the resource input concentrations (I_{in} , R_{in}). This model exercise predicts that *Synechococcus* will dominate at high nitrate input concentrations, whereas the two species will coexist at low nitrate input concentrations. The four competition experiments between *Cyanothece* and *Synechococcus* corroborate these model predictions. The experiment that led to coexistence falls within the coexistence region, while the three other experiments fall in the dominance region of *Synechococcus* (Fig. 8B). Strikingly, the model simulations predict that there is no region of dominance for the nitrogen-fixing *Cyanothece*. Even at very low nitrate input concentrations, the model predicts coexistence (Fig. 8B; note the difference with Fig. 1). According to the simulations, the release of fixed nitrogen by *Cyanothece* facilitates its competitors and thereby favors their coexistence instead of competitive exclusion. This intricate balance between competition and facilitation offers an intriguing explanation for the observa-

tion that unicellular nitrogen-fixing cyanobacteria are often subordinate or co-dominant species in phytoplankton communities (Zehr et al. 2001; Mazard et al. 2004; Montoya et al. 2004), but seldom fully dominate the ecosystem.

To what extent can these laboratory findings be translated to open ocean ecosystems? Both the population densities and nitrate input concentrations in the laboratory chemostats were several orders of magnitude higher than the low population densities and nitrate concentrations in the oligotrophic ocean. This might suggest that the relevance of our chemostat experiments is limited. Under light-limited conditions, however, phytoplankton production scales inversely with mixed-layer depth (Petersen et al. 1997; Huisman 1999; Diehl et al. 2002). This scaling rule implies that, if mixed-layer depth is raised by three orders of magnitude, from the laboratory scale of 5 cm to a mixed-layer depth of 50 m, then the corresponding population densities and nitrogen input concentrations will become three orders of magnitude lower. Although this scaling argument offers only a first approximation, it indicates that, after suitable rescaling, the regions of coexistence and competitive exclusion in Fig. 8B will be highly relevant for open ocean ecosystems as well.

Our experiments focused on nitrogen and light as limiting factors, whereas other nutrients, such as phosphorus and iron, were supplied to the chemostats in saturating concentrations. In various oceanic regions, however, phosphorus and iron limitation have a major impact on phytoplankton production (Martin et al. 1994; Wu et al. 2000) and on the growth and distribution of nitrogen-fixing cyanobacteria (Sañudo-Wilhelmy et al. 2001; Kustka et al. 2003; Mills et al. 2004). Nitrogen fixation is even held responsible for shifts from a primarily nitrogen-limited ocean to an ocean ecosystem on the edge of nitrogen and phosphorus limitation (Karl et al. 1995, 1997; Tyrrell 1999). This mechanism is analogous to our experiments, where nitrogen excretion by *Cyanothece* shifted the phytoplankton mixture from a nitrogen-limited system to a system on the edge of nitrogen and light limitation. Our findings illustrate that the prevalence of nitrogen-fixing cyanobacteria should be interpreted not only in terms of nitrogen : phosphorus ratios, but also in terms of light availability (Fig. 8). For instance, seasonal variations in solar irradiance are likely to affect the relative abundance of nitrogen-fixing cyanobacteria. The interplay between nitrogen, phosphorus, iron, and light in controlling the competition between nitrogen-fixing cyanobacteria and other phytoplankton species deserves further attention in future studies.

In conclusion, our model and experiments demonstrate that competition between nitrogen-fixing cyanobacteria and other phytoplankton species can be accurately predicted at different nitrate and light levels. The model and experiments further show that several physiological traits, like the switch between nitrate assimilation and nitrogen fixation, the light dependence of nitrogen fixation, and the rate of nitrogen release, play a major role in the population dynamics of nitrogen-fixing cyanobacteria. In particular, high rates of nitrogen release by nitrogen-fixing cyanobacteria facilitate the growth of other phytoplankton and thus promote the coexistence of nitrogen-fixing and

non-nitrogen-fixing species. As a next step, these competition models can now be embedded in ecosystem models to improve the prediction of the distribution and abundances of nitrogen-fixing cyanobacteria and their effects on the nitrogen and carbon cycles of the oceans.

References

- AGAWIN, N. S. R., S. AGUSTÍ, AND C. M. DUARTE. 2002. Abundance of Antarctic picophytoplankton and their response to light and nutrient manipulation. *Aquat. Microb. Ecol.* **29**: 161–172.
- BOUSHABA, K., AND M. PASCUAL. 2005. Dynamics of the 'echo' effect in a phytoplankton system with nitrogen fixation. *Bull. Math. Biol.* **67**: 487–507.
- CAMPBELL, C., H. TAKEYAMA, AND A. MITSUI. 1994. Cyclic synthesis of messenger RNA from nitrogenase *nifH* gene in synchronous cultures of marine unicellular cyanobacterium, *Synechococcus* sp. strain Miami BG043511. *J. Mar. Biotech.* **2**: 39–43.
- CAPONE, D. G. 2000. The marine nitrogen cycle, p. 455–493. *In* D. L. Kirchman [ed.], *Microbial ecology of the oceans*. Wiley.
- , M. D. FERRIER, AND E. J. CARPENTER. 1994. Amino acid cycling in colonies of the planktonic marine cyanobacterium *Trichodesmium thiebautii*. *Appl. Environ. Microbiol.* **60**: 3989–3995.
- , J. P. ZEHR, H. W. PAERL, B. BERGMAN, AND E. J. CARPENTER. 1997. *Trichodesmium*: A globally significant marine cyanobacterium. *Science* **276**: 1221–1229.
- DIEHL, S., S. BERGER, R. PTACNIK, AND A. WILD. 2002. Phytoplankton, light, and nutrients in a gradient of mixing depths: Field experiments. *Ecology* **83**: 399–411.
- FALKOWSKI, P. G. 1997. Evolution of the nitrogen cycle and its influence on the biological sequestration of CO₂ in the ocean. *Nature* **387**: 272–275.
- GALLON, J. R., AND OTHERS. 2002. Maximum rates of N₂ fixation and primary production are out of phase in a developing cyanobacterial bloom in the Baltic Sea. *Limnol. Oceanogr.* **47**: 1514–1521.
- GRASSHOFF, K. 1967. *Methods of seawater analysis*. Verlag Chemie, Weinheim.
- GROVER, J. P. 1997. *Resource competition*. Chapman and Hall.
- GRUBER, N., AND J. L. SARMIENTO. 1997. Global patterns of marine nitrogen fixation and denitrification. *Glob. Biogeochem. Cycles* **11**: 235–266.
- HEALEY, F. P. 1985. Interacting effects of light and nutrient limitation on the growth rate of *Synechococcus linearis* (Cyanophyceae). *J. Phycol.* **21**: 134–146.
- HELDER, W., AND R. T. P. DE VRIES. 1979. An automatic phenol-hypochlorite method for the determination of ammonia in sea- and brackish waters. *Neth. J. Sea Res.* **13**: 154–160.
- HOLL, C. M., AND J. P. MONTROYA. 2005. Interactions between nitrate uptake and nitrogen fixation in continuous cultures of the marine diazotroph *Trichodesmium* (Cyanobacteria). *J. Phycol.* **41**: 1178–1183.
- HUISMAN, J. 1999. Population dynamics of light-limited phytoplankton: Microcosm experiments. *Ecology* **80**: 202–210.
- , R. R. JONKER, C. ZONNEVELD, AND F. J. WEISSING. 1999. Competition for light between phytoplankton species: experimental tests of mechanistic theory. *Ecology* **80**: 211–222.
- , J. SHARPLES, J. M. STROOM, P. M. VISSER, W. E. A. KARDINAAL, J. M. H. VERSPAGEN, AND B. SOMMEIJER. 2004. Changes in turbulent mixing shift competition for light between phytoplankton species. *Ecology* **85**: 2960–2970.
- , AND F. J. WEISSING. 1994. Light-limited growth and competition for light in well-mixed aquatic environments: An elementary model. *Ecology* **75**: 507–520.
- , AND ———, 1995. Competition for nutrients and light in a well-mixed water column: A theoretical analysis. *Am. Nat.* **146**: 536–564.
- IKEMOTO, H., AND A. MITSUI. 1994. Diazotrophic synchronous growth of marine unicellular cyanobacterium, *Synechococcus* sp. strain Miami BG 043511, under aerobic and microaerobic/anaerobic conditions. *Microbiology* **140**: 2153–2158.
- JONKER, R. R., J. T. MEULEMANS, G. B. J. DUBELAAR, M. F. WILKINS, AND J. RINGELBERG. 1995. Flow cytometry: A powerful tool in analysis of biomass distributions in phytoplankton. *Water Sci. Technol.* **32**: 177–182.
- KARL, D. M., R. LETELIER, D. HEBEL, L. TUPAS, J. DORE, J. CHRISTIAN, AND C. WINN. 1995. Ecosystem changes in the North Pacific subtropical gyre attributed to the 1991–92 El Niño. *Nature* **373**: 230–234.
- KARL, D., R. LETELIER, L. TUPAS, J. DORE, J. CHRISTIAN, AND D. HEBEL. 1997. The role of nitrogen fixation in biogeochemical cycling in the subtropical North Pacific Ocean. *Nature* **388**: 533–538.
- KLAUSMEIER, C. A., E. LITCHMAN, T. DAUFRESNE, AND S. A. LEVIN. 2004. Optimal nitrogen-to-phosphorus stoichiometry of phytoplankton. *Nature* **429**: 171–174.
- KUSTKA, A. B., S. A. SANUDO-WILHELMY, E. J. CARPENTER, D. G. CAPONE, J. BURNS, AND W. G. SUNDA. 2003. Iron requirements for dinitrogen- and ammonium-supported growth in cultures of *Trichodesmium* (IMS 101): Comparison with nitrogen fixation rates and iron:carbon ratios of field populations. *Limnol. Oceanogr.* **48**: 1869–1884.
- LAROCHE, J., AND E. BREITBARTH. 2005. Importance of the diazotrophs as a source of new nitrogen in the ocean. *J. Sea Res.* **53**: 67–91.
- LITCHMAN, E., AND C. A. KLAUSMEIER. 2001. Competition of phytoplankton under fluctuating light. *Am. Nat.* **157**: 170–187.
- MARTIN, J. H., AND OTHERS. 1994. Testing the iron hypothesis in ecosystems of the equatorial Pacific Ocean. *Nature* **371**: 123–129.
- MAZARD, S. L., N. J. FULLER, K. M. ORCUTT, O. BRIDLE, AND D. J. SCANLAN. 2004. PCR analysis of the distribution of unicellular cyanobacterial diazotrophs in the Arabian Sea. *Appl. Environ. Microbiol.* **70**: 7355–7364.
- MILLS, M. M., C. RIDAME, M. DAVEY, J. LA ROCHE, AND R. J. GEIDER. 2004. Iron and phosphorus co-limit nitrogen fixation in the eastern tropical North Atlantic. *Nature* **429**: 292–294.
- MITSUI, A., AND S. CAO. 1988. Isolation and culture of marine nitrogen-fixing unicellular cyanobacteria *Synechococcus*. *Methods Enzymol.* **167**: 105–113.
- , S. KUMAZAWA, A. TAKAHASHI, H. IKEMOTO, S. CAO, AND T. ARAI. 1986. Strategy by which nitrogen-fixing unicellular cyanobacteria grow photoautotrophically. *Nature* **323**: 720–722.
- MONTROYA, J. P., C. M. HOLL, J. P. ZEHR, A. HANSEN, T. A. VILLAREAL, AND D. G. CAPONE. 2004. High rates of N₂ fixation by unicellular diazotrophs in the oligotrophic Pacific Ocean. *Nature* **430**: 1027–1032.
- MULHOLLAND, M. R. 2007. The fate of nitrogen fixed by diazotrophs in the ocean. *Biogeosciences* **4**: 37–51.
- , AND P. W. BERNHARDT. 2005. The effect of growth rate, phosphorus concentration, and temperature on N₂ fixation, carbon fixation, and nitrogen release in continuous cultures of *Trichodesmium* IMS101. *Limnol. Oceanogr.* **50**: 839–849.

- , P. W. BERNHARDT, C. A. HEIL, D. A. BRONK, AND J. M. O'NEIL. 2006. Nitrogen fixation and release of fixed nitrogen by *Trichodesmium* spp. in the Gulf of Mexico. *Limnol. Oceanogr.* **51**: 1762–1776.
- , K. OHKI, AND D. G. CAPONE. 2001. Nutrient controls on nitrogen uptake and metabolism by natural populations and cultures of *Trichodesmium* (Cyanobacteria). *J. Phycol.* **37**: 1001–1009.
- OHLENDIECK, U., K. GUNDERSEN, M. MEYERHÖFER, P. FRITSCHÉ, K. NACHTIGALL, AND B. BERGMANN. 2007. The significance of nitrogen fixation to new production during early summer in the Baltic Sea. *Biogeosciences* **4**: 63–73.
- PASSARGE, J., S. HOL, M. ESCHER, AND J. HUISMAN. 2006. Competition for nutrients and light: stable coexistence, alternative stable states, or competitive exclusion? *Ecol. Monogr.* **76**: 57–72.
- PETERSEN, J. E., C. C. CHEN, AND W. M. KEMP. 1997. Scaling aquatic primary productivity: experiments under nutrient- and light-limited conditions. *Ecology* **78**: 2326–2338.
- RABOUILLE, S., M. STAAL, L. J. STAL, AND K. SOETAERT. 2006. Modeling the dynamic regulation of nitrogen fixation in the cyanobacterium *Trichodesmium* sp. *Appl. Environ. Microbiol.* **72**: 3217–3227.
- RAVEN, J. A. 1998. Small is beautiful: The picophytoplankton. *Funct. Ecol.* **21**: 503–513.
- RHEE, G.-Y., AND I. J. GOTHAM. 1981. The effect of environmental factors on phytoplankton growth: light and the interactions of light with nitrate limitation. *Limnol. Oceanogr.* **26**: 649–659.
- SANUDO-WILHELMY, S. A., AND OTHERS. 2001. Phosphorus limitation of nitrogen fixation by *Trichodesmium* in the central Atlantic Ocean. *Nature* **411**: 66–69.
- SMITH, V. H. 1983. Low nitrogen to phosphorus ratios favor dominance by blue-green algae in lake phytoplankton. *Science* **221**: 669–671.
- SOETAERT, K., V. DECLIPPELE, AND P. HERMAN. 2002. FEMME, a flexible environment for mathematically modelling the environment. *Ecol. Model.* **151**: 177–193.
- SOMMER, U. 1986. Nitrate- and silicate competition among Antarctic phytoplankton. *Mar. Biol.* **91**: 345–351.
- . 1993. Phytoplankton competition in Plußsee: A field test of the resource-ratio hypothesis. *Limnol. Oceanogr.* **38**: 838–845.
- . 1994. The impact of light intensity and daylength on silicate and nitrate competition among marine phytoplankton. *Limnol. Oceanogr.* **39**: 1680–1688.
- STAAL, M., S. TE LINTEL HEKKERT, P. HERMAN, AND L. J. STAL. 2002. Comparison of models describing light dependence of N₂ fixation in heterocystous cyanobacteria. *Appl. Environ. Microbiol.* **68**: 4679–4683.
- STOMP, M., J. HUISMAN, L. VÖRÖS, F. R. PICK, M. LAAMANEN, T. HAVERKAMP, AND L. J. STAL. 2007. Colourful coexistence of red and green picocyanobacteria in lakes and seas. *Ecol. Lett.* **10**: 290–298.
- , AND OTHERS. 2004. Adaptive divergence in pigment composition promotes phytoplankton biodiversity. *Nature* **432**: 104–107.
- TILMAN, D. 1977. Resource competition between planktonic algae: an experimental and theoretical approach. *Ecology* **58**: 338–348.
- . 1982. Resource competition and community structure. Princeton Univ. Press.
- TYRRELL, T. 1999. The relative influences of nitrogen and phosphorus on oceanic primary production. *Nature* **400**: 525–531.
- VELDHUIS, M. J. W., AND G. W. KRAAY. 2004. Phytoplankton in the subtropical Atlantic Ocean: Towards a better assessment of biomass and composition. *Deep-Sea Res. I* **51**: 507–530.
- WATERBURY, J. B., AND R. RIPPKA. 1989. Order *Chroococcales* Wettstein 1924, emend. Rippka et al. 1979, p. 1728–1746. *In* J. T. Staley, M. P. Bryant, N. Pfennig and J. G. Holt [eds.], *Bergey's manual of systematic bacteriology*, vol. 3. Williams and Wilkins.
- WU, J. F., W. SUNDA, E. A. BOYLE, AND D. M. KARL. 2000. Phosphate depletion in the western North Atlantic Ocean. *Science* **289**: 759–762.
- WYATT, J. T., AND J. K. G. SILVEY. 1969. Nitrogen fixation by *Gloeocapsa*. *Science* **165**: 908–909.
- ZEHR, J. P., AND OTHERS. 2001. Unicellular cyanobacteria fix N₂ in the subtropical North Pacific Ocean. *Nature* **412**: 635–638.
- ZEVENBOOM, W., J. VAN DER DOES, K. BRUNING, AND L. R. MUR. 1981. A non-heterocystous mutant of *Aphanizomenon flos-aquae*, selected by competition in light-limited continuous culture. *FEMS Microbiol. Lett.* **10**: 11–16.

Received: 23 January 2007

Accepted: 29 April 2007

Amended: 13 May 2007